# THE STRUCTURES OF THE GROUP 15 ELEMENT(III) HALIDES AND HALOGENOANIONS

GEORGE A. FISHER and NICHOLAS C. NORMAN

Department of Chemistry, The University of Newcastle upon Tyne, Newcastle upon Tyne, NE1 7RU, United Kingdom



## I. Introduction

This chapter deals with the solid-state structures of the element(III) halides and halogenoanions of arsenic, antimony, and bismuth with brief mention of some compounds of phosphorus where relevant. A

number of related topics will not be considered here; these include lower oxidation state halides, or subhalides, element(V) compounds, and mixed oxidation state species. It does not attempt to be fully comprehensive but instead highlights important structural classes and references a number of representative examples. Coordination complexes involving element halides or halogenoanions and neutral two-electron donor ligands L (or multidentate $L_n$), although a large and rapidly expanding field, and a number of cationic species such as $[Sb_2F_4]^{2+}$ and $[Sb_6F_{13}]^{5+}$ (*1*) will also not be considered.

This area has not been reviewed extensively before although Davidovich and Buslaev (*2*) have considered the coordination chemistry of bismuth in a general way, in which the structures of halides and halogenoanions are featured. Sawyer and Gillespie (*3*) have commented previously upon the stereochemistry of antimony(III) halides (mostly fluorides).

The element trihalides will be considered first, followed by the many classes of anionic structures that are known. Finally, a section on bonding and on the various ideas that have been used to rationalize some of the observed trends is included.

## II. Element Trihalides, $EX_3$

The structures of the element trihalides $EX_3$ are covered in a number of textbooks on structural inorganic chemistry (*4, 5*), and these will not be discussed in great detail here. It is, however, worth mentioning some of the salient structural features. In most cases, a molecular trigonal pyramidal $EX_3$ unit consistent with VSEPR theory predictions is readily apparent in the solid-state structure, although there are usually a number of fairly short intermolecular contacts or secondary bonds present. A general description of the structures as molecularly covalent but as having a tendency toward macromolecular or polymeric networks is therefore reasonable. Only in the case of the fluorides is an ionic model appropriate.

In $SbF_3$ (*6*) the antimony atom is bonded to three fluorines (av. Sb–F, 1.92 Å) in a trigonal pyramidal arrangement with three other fluorines at greater distances (av. 2.61 Å) approximately *trans* to the primary Sb–F bonds, such that the overall coordination geometry around the antimony center is that of a distorted octahedron. In bismuth trifluoride, a primary $BiF_3$ trigonal pyramid is much less evident and the bismuth atom has a larger coordination number with eight nearest neighbors at distances ranging from 2.233 to 2.503 Å in a bicapped

trigonal prismatic geometry; a ninth and more distant fluorine (3.105 Å) is present in the remaining capping site (*7*).

The solid-state structures of $SbCl_3$ (*8*) and $\beta$-$SbBr_3$ (*9*) are isomorphous with $BiF_3$, although in both cases the primary $SbX_3$ pyramid is clearly discernable. Thus in $SbCl_3$ there are three short Sb–Cl bonds (av., 2.359 Å), with five longer bonds ranging from 3.457 to 3.736 Å, whereas in $\beta$-$SbBr_3$ the three short Sb–Br bonds average 2.49 Å, with the longer distances at 3.6 Å and greater. The structure of $BiCl_3$ (*10*) is very similar (although not strictly isomorphous) with three short Bi–Cl bonds (av., 2.500 Å) and five longer distances of 3.216 to 3.450 Å, as shown in Fig. 1.

The compound $\alpha$-$SbBr_3$ (*11*) is isomorphous with $AsBr_3$ (*12*), and in both cases the $EX_3$ pyramid is also evident, although, unlike the structures mentioned above, there are only three short intermolecular contacts. For $\alpha$-$SbBr_3$ the primary and secondary Sb–Br bonds average 2.50 and 3.75 Å, respectively, whereas in $AsBr_3$ the corresponding As–Br distances are 2.36 and 3.77 Å.

Bismuth tribromide also exists as two modifications (*13*). In $\alpha$-$BiBr_3$ the bismuth atom is bonded to three bromines (av., 2.663 Å) with a trigonal pyramidal coordination geometry, with three longer secondary bonds (av., 3.316 Å) approximately *trans* to the primary bonds, as shown in Fig. 2; one phase of $SbI_3$ (*14*) is isomorphous with corresponding average distances of 2.765 and 3.675 Å. In $\beta$-$BiBr_3$ a trigonal pyra-

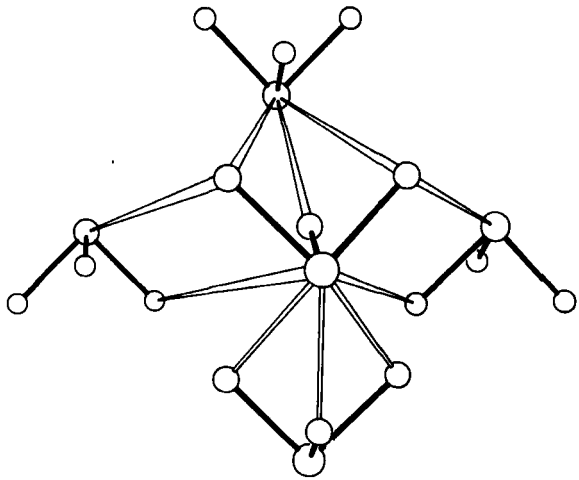

FIG. 1. Part of the structure of $BiCl_3$, showing the three short and five long Bi—Cl bonds about the bismuth center as filled and open bonds, respectively.

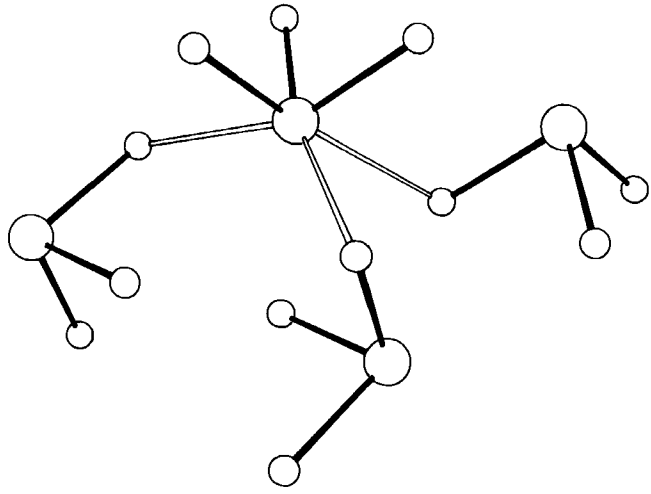

FIG. 2. Part of the structure of $\alpha$-$BiBr_3$ showing the three short and three long Bi—Br bonds as filled and open bonds, respectively.

midal $BiBr_3$ unit is not evident and the bismuth resides in a fairly regular octahedron of bromines for which the average Bi–Br distance is 2.81 Å, intermediate between the primary and secondary bond distances in $\alpha$-$BiBr_3$.

Octahedral coordination is also encountered in the structures of a second phase of $SbI_3$ (*15*), which is isomorphous with $AsI_3$ (*16*) and $BiI_3$ (*15*), and these three structures provide an interesting comparison in terms of the relative lengths of the primary and secondary bonds. Thus the structures can be viewed as comprising a hexagonally close-packed array of iodines in which $\frac{1}{3}$ of the octahedral holes (strictly $\frac{2}{3}$ of the octahedral holes in alternate layers) are occupied by As, Sb, or Bi. In $AsI_3$ there are three short As–I bonds (2.591 Å) and three longer bonds (3.467 Å), whereas in $BiI_3$ all six Bi–I distances are equal at 3.1 Å; in $SbI_3$ the situation is intermediate, with short and long Sb–I bonds of 2.868 and 3.32 Å, respectively.

Clearly there are a number of interesting trends that are apparent here and that require explanation. Table I lists the approximate differences between the primary and the secondary E–X bond lengths ($\Delta$) for the element trihalides $EX_3$; common superscripts reflect isomorphous (or nearly so) structures for which a comparison is particularly appropriate.

Before proceeding, however, the terms primary bond and secondary bond should be defined more thoroughly. This matter, and the concept

TABLE I

APPROXIMATE DIFFERENCES (TO THE NEAREST 0.05 Å) BETWEEN THE LENGTHS OF THE PRIMARY AND SECONDARY E—X BONDS (Δ) FOR THE ELEMENT TRIHALIDES $EX_3$[a]

| E—F | Δ (Å) | E—Cl | Δ (Å) | E—Br | Δ (Å) | E—I | Δ (Å) |
|---|---|---|---|---|---|---|---|
| | | | | As—Br | 1.40¶ | As—I | 0.90§ |
| Sb—F | 0.70 | Sb—Cl | 1.25* | Sb—Br | 1.25¶ (α), 1.10* (β) | Sb—I | 0.45§, 0.91# |
| Bi—F | —* | Bi—Cl | 0.85* | Bi—Br | 0.65# (α), 0 (β) | Bi—I | 0§ |

[a] Common superscripts indicate isomorphous or nearly isomorphous structures.

of secondary bonding in general, has been addressed by Alcock (*17*), wherein a primary bond is taken as a normal covalent bond with a bond length within usual ranges, whereas a secondary bond is a significantly longer interaction, although considerably less than the sum of the van der Waals radii for the two elements concerned. Moreover, it is usually observed that secondary bonds lie approximately *trans* to primary bonds and that there is a strong correlation between the *trans*-related primary and secondary bond distances such that, as the secondary distance gets shorter, the primary distance gets longer; when the two distances become equal (or nearly so) the distinction between primary and secondary is lost; i.e., $\Delta = 0$. This latter feature, or *trans* effect as it is sometimes called, has been commented upon in detail by Alcock (*17, 18*) and Sheldrick (*19*) and is consistent with the idea that the acceptor orbitals on the $EX_3$ unit, which are responsible for the presence of secondary bonding or, more generally, element center Lewis acidity, are the E–X $\sigma^*$-orbitals (as opposed to a more conventional explanation based on the use of vacant *d* orbitals), a matter that has been discussed in some detail and which will not be reiterated here (*17, 20*).

Similar *trans* effect correlations have also been observed for related selenium and tellurium halide complexes by Knop and coworkers and by Krebs and Ahlers (*19*); a number of structural similarities between group 16 halides and halogenoanions are evident and these are mentioned where appropriate in the following section.

One thing that is immediately clear from Table I is that for a given halide there is a strong tendency for the difference between the primary and the secondary bond lengths to decrease on moving from As to Sb to Bi, this being particularly well illustrated in the isomorphous series of $EI_3$ structures.

Furthermore, for a given group 15 element, there is tendency for Δ to decrease on moving to heavier halides as is clear from the structures of $BiCl_3$, $BiBr_3$, and $BiI_3$, although the fluorides are an obvious exception here. This last point is most likely a result of a large E–F electro-

negativity difference (two to three times greater than that between other bond pairs in this table using modified Pauling electronegativities), and the structures are probably best considered as ionic, for which equal or nearly equal interionic distances are not unexpected; covalent bonding and hence a discussion of primary and secondary bonds are therefore not really appropriate here.

For all the other cases in which the electronegativity differences are much smaller, covalent bonding is appreciable and this is reflected in the observed bond localization in many of the structures, i.e., the appearance of a definite $EX_3$ pyramid. The remaining trend, therefore, is that, in situations in which covalent bonding is important, i.e., excluding the fluorides, the secondary bonding interactions become more pronounced on moving to both heavier group 15 elements and to heavier halides and therefore that $\Delta$ approaches zero. In $BiI_3$ and $\beta$-$BiBr_3$ all Bi–I and Bi–Br distances are equal and the limit of $\Delta = 0$ is reached. This is, in fact, quite a general observation in that secondary bonding interactions tend to increase (as defined by a decreasing $\Delta$) as the electronegativity of the elements decrease and, importantly, as the element size increases (*17, 18, 20*). In $BiI_3$, therefore, it is an equivalence of primary and secondary bonding interactions that results in a regular octahedral coordination of six iodines around the bismuth center; the structure is not this way because it is ionic, as is sometimes stated, because the electronegativity difference between bismuth and iodine is far too small to result in ionic bonding. A complementary explanation for $BiI_3$ and $\beta$-$BiBr_3$ is that, as the element electronegativities become similar and fall within the range typical of metalloids, metalloid-type structures are encountered, i.e., polymeric or macromolecular solid-state structures with equal bond distances and a delocalized but covalent bonding scheme.

Another feature, and one that will be met again in many of the structures of the anions to follow, is that, in $\beta$-$BiBr_3$ and $BiI_3$, the lone pair of electrons associated with the bismuth(III) center is stereochemically inactive. A number of these points will be returned to in Section IV.

## III. Element(III) Halogenoanions

The element halogenoanions are a structurally diverse group of compounds and will be considered in the following sections according to common structural types. There is no unique way in which to do this, but, throughout, the relationships between the various forms will be highlighted.

## A. $[EX_4]^-$

The simplest species results from formal addition of one halide anion to one $EX_3$ molecule to give the $[EX_4]^-$ anion. Such species usually dimerize or polymerize, but a genuine example of a discrete mononuclear species is found in the structure of $[Et_4N][PCl_4]$ (**1**) (*21*). The structure is shown in Fig. 3 and the coordination geometry around the phosphorus center may be adequately described as an equatorially vacant, trigonal bipyramid. Such a structure is predicted by VSEPR rules for an $AX_4E$ (E = lone pair here) species, but it is worth commenting on the inequivalence of the axial P–Cl bond lengths. The equatorial P–Cl distances average 2.046 Å, whereas the distances to the axial chlorines are 2.118 and 2.850 Å. This is fully consistent with the $\sigma^*$-bonding model outlined above and will be considered again in Section IV. Thus, the structure of **1** may be viewed as an adduct of $PCl_3$ with $Cl^-$ in which the chloride is approaching *trans* to Cl(2), resulting in a slight lengthening of this bond.

A second structure which should be considered here is that of $[Pr^n_4N][PBr_4]$ (**2**) (*22*), shown in Fig. 4. The essential unit is similar to that in **1**, although the axial P–Br bonds are much more similar in length, but there is clearly a degree of dimerization present as evidenced by the P–Br(1′) distance of 3.460 Å, which, although much longer than the corresponding primary distance [P–Br(1), 2.527 Å], is certainly smaller than the sum of the van der Waals radii for P and Br (3.85 Å). Note also that the Br(1′)–P–Br(4) angle of 167.9° places Br(1′) almost *trans* to Br(1), and the geometry around the phosphorus center can

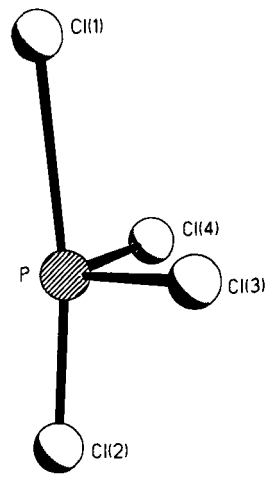


FIG. 3. The structure of $[PCl_4]^-$ in **1**.

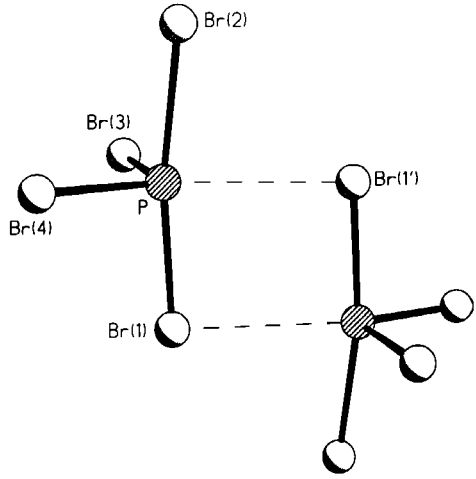


FIG. 4. The structure of $[PBr_4]^-$ in **2**.

therefore be considered as a five-coordinate square-based pyramid. The fact that the bromide shows the beginnings of five-coordination as opposed to the four-coordinate chloride complex is consistent with the increasing importance of secondary bonding for the heavier halides as mentioned in the previous section.

## B. $[E_2X_8]^{2-}$

The structure of **2** is clearly on the borderline between being a monomer and being a dimer, and in this section compounds for which a dimeric formulation is unambiguous will be considered. Clearly there exists, in principle at least, a continuum from a weakly bound to a more strongly bound to a symmetrically bound dimer, extremes of which are shown in the diagrams **A** and **B**, and any distinction that is made will necessarily be somewhat arbitrary.

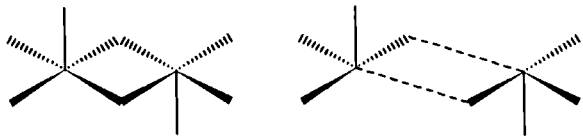

**A** **B**

With the above caveat in mind, some examples of complexes for which the dimeric formula $[E_2X_8]^{2-}$ is clearly appropriate are $[PhMeNH_2]_2[As_2Cl_8]$ (**3**) (*23*), $[Ph_4P]_2[As_2Br_8]$ (**4**) (*24*), $[Pr_4^nN]_2[As_2Br_8]$ (**5**) (*24*), $[Pr_4^nN]_2[As_2I_8]$ (**6**) (*25*), $[Ph_4P]_2[Sb_2I_8]$ (**7**) (*26*), $[Bu^tNH_3]_2$

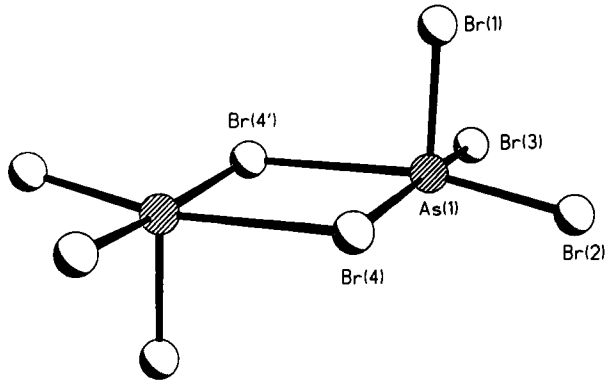


FIG. 5. The structure of $[As_2Br_8]^{2-}$ in **5**.

$[Sb_2Cl_8]$ (**8**) (*27*), and $[BiCl_2(18\text{-crown-6})][Bi_2Cl_8]$ (**9**) (*28*); a view of **5** is shown in Fig. 5.

A couple of points deserve further comment. In all structures the element center is five-coordinate and the overall structure can be described as edge-shared, bis-square-based pyramidal with the apical halides *anti* rather than *syn;* moreover, the halide bridges are fairly symmetric and a representation as in **A** is appropriate. Furthermore, the structures of **5** and **6** are isomorphous with the phosphorus bromide complex **2**, which provides a further illustration of the trend toward increasing secondary bonding for arsenic and antimony as opposed to phosphorus. This statement about secondary bonding can be restated as a trend toward increasing Lewis acidity on progressing to the heavier elements in group 15, and it is therefore interesting to note that the structures of **4** and **7** are not isomorphous and that in **7** there is a close contact between a phenyl ring of the $[Ph_4P]^+$ cation and the vacant site at the antimony center, which is absent in the structure of **4**.

A further example of *anti* $[E_2X_8]^{2-}$ is $[Pr_4^nN]_2[Sb_2Cl_8]$ (**10**) (*29*) (not isomorphous with **2, 5,** or **6**), in which there are two crystallographically independent anions, one of which has fairly asymmetric Sb–Cl–Sb bridges (2.716 and 3.111 Å as opposed to 2.794 and 2.961 Å), but of more interest is the structure of $[Bu_4^nN]_2[Sb_2Cl_8]$ (**11**) (*29*), which has a *syn* arrangement of apical chlorides as shown in **C**; the Sb–Cl–Sb bridges are quite symmetric in this case.

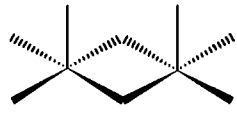

**C**

C. $[\{EX_4\}_n]^{n-}$

Probably the most commonly encountered form of the $[EX_4]^-$ unit is as a one-dimensional polymer, which may be represented as $[\{EX_4\}_n]^{n-}$ (although in the formulas to follow, $[EX_4]$ is simpler), in which the coordination about the group 15 element has increased to six and the geometry is approximately octahedral. Examples include $[C_5H_5NH][AsBr_4]$ (**12**) (*30*), $[C_5H_5NH][AsI_4]$ (**13**) (*31*), $[C_5H_5NH][SbCl_4]$ (**14**) (*32*), $[Mg(MeCN)_6][SbCl_4]_2$ (**15**) (*33*), $[Et_2NH_2][BiCl_4]$ (**16**) (*34*), $[Fe(\eta\text{-}C_5H_5)_2][BiCl_4]$ (**17**) (*35*), [2-picolinium][$BiBr_4$] (**18**) (*36*), and [2-picolinium][$BiI_4$] (**19**) (*36*). The structure of a section of the polymer in **17** is shown in Fig. 6 and, more generally, in **D**, from which it is apparent that adjacent $E_2(\mu\text{-}X)_2$ planes are perpendicular and that the terminal or nonbridging halides are always *cis*.

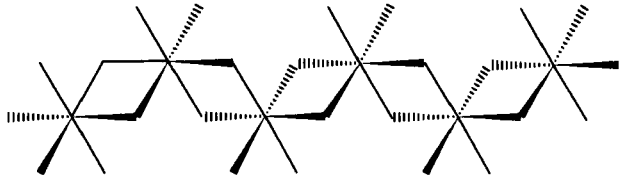

**D**

There is a considerable variation in the degree of bridge asymmetry present in these structures and it is often found that alternate bridging units have quite different degrees of asymmetry. For example, in **12**, the relevant distances are 2.688 and 3.130 Å for one $As_2(\mu\text{-}Br)_2$ unit and 2.690 and 3.129 Å for the adjacent unit (i.e., both are the same within experimental error). This is clearly a polymeric structure and the average difference between the primary and the secondary bond lengths is 0.440 Å, a value that is fairly typical of most structures. In

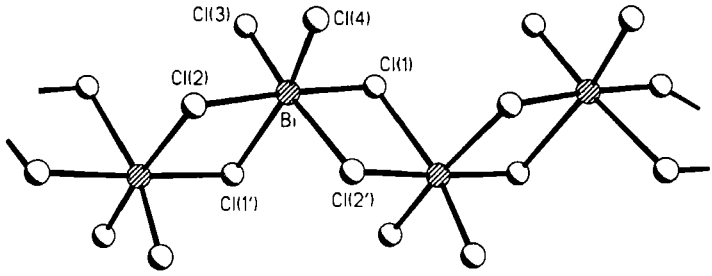


FIG. 6. Part of the polymeric structure of $[\{BiCl_4\}_n]^{n-}$ in **17**.

**15**, however, the difference in asymmetry between alternate bridging units is considerable, the relevant pairs of distances being 2.822/3.006 Å (difference, 0.184) and 2.433/3.580 Å (difference, 1.147). In this latter case, a description of the structure as a loosely bound polymer of dimers is more appropriate.

Before leaving this section, mention should be made of a number of other structures that are also polymeric but that have rather different overall arrangements of the monomeric units. In $Na[SbF_4]$ (**20**) (*37*) a basic $[SbF_4]^-$ unit is clearly discernable, with Sb–F distances from 1.94 to 2.07 Å and two secondary interactions at 2.68 and 2.86 Å, such that the overall structure can be described as two linked one-dimensional polymeric chains, as shown in **E**.

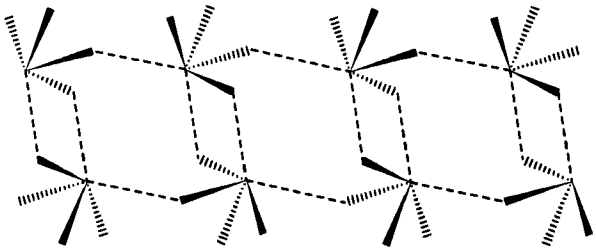

**E**

In $K[SbF_4]$ (**21**) (*38*) the $[SbF_4]^-$ unit is less distinct, there being three short Sb–F distances together with two longer and one longer still. Some mixed chloro–fluoro compounds are also known. These include $K[SbClF_3]$ (**22**) (*39*) and $Cs[SbClF_3]$ (**23**) (*40*), the former having a structure in which the antimony center is bonded to three fluorines (av., 1.95 Å) with three much longer contacts to three chlorine atoms (av., 3.12 Å) and with an arrangement around the antimony center as shown in **F**, which can be described as a $C_{3v}$ distorted octahedron. The structure is perhaps best thought of as comprising $SbF_3$ molecules together with chloride and potassium ions.

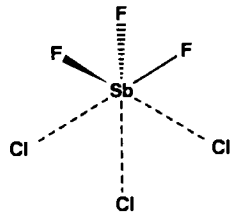

Finally, in the structure of $[NH_4][BiF_4]$ (**24**) (*41*), for which an ionic description is appropriate, the bismuth center is coordinated by nine fluorines in a fashion similar to that found in the structure of $BiF_3$.

## D. $[E_4X_{16}]^{4-}$

Anions of the formula $[E_4X_{16}]^{4-}$ can be thought of either as tetramers of $[EX_4]^-$ or, in some cases, as dimers of $[E_2X_8]^{2-}$. Three types of structure have been characterized, the first of which corresponds to the description as a dimer of $[E_2X_8]^{2-}$ units. Examples include $[HL]_4[Sb_4Br_{16}]$ (L = 2-amino-1,3,4-thiadiazole) (**25**) (*42*), $[Mg(MeCN)_6]_2[Bi_4Cl_{16}]$ (**26**) (*43*), and $[Fe(\eta\text{-}C_5H_5)_2]_4[Bi_4Br_{16}]$ (**27**) (*44*). A view of **27** is shown in Fig. 7 and a line diagram is shown in **G**. Any perspective from **G** has been omitted but one $[E_2X_8]^{2-}$ is highlighted to indicate how the structure can be viewed as a dimer of *syn* $[E_2X_8]^{2-}$ units. An alternative description, which will be useful in a later discussion of higher nuclearity clusters, is an $[E_2X_{10}]^{4-}$ edge-shared bioctahedral structure, itself discussed later, to which a neutral $E_2X_6$ unit has been added, as is illustrated in **H**, or to which two face capping $EX_3$ units have been added, as shown in **I**. The overall structure is analogous to one form of $TeI_4$.

A second structural type is found in $[Et_4N]_4[Sb_4Cl_{16}]$ (**28**) (*29*), which is shown in Fig. 8. This structure can also be thought of in terms of a dimerization of *syn* $[E_2X_8]^{2-}$ units but in which the E–E vectors are

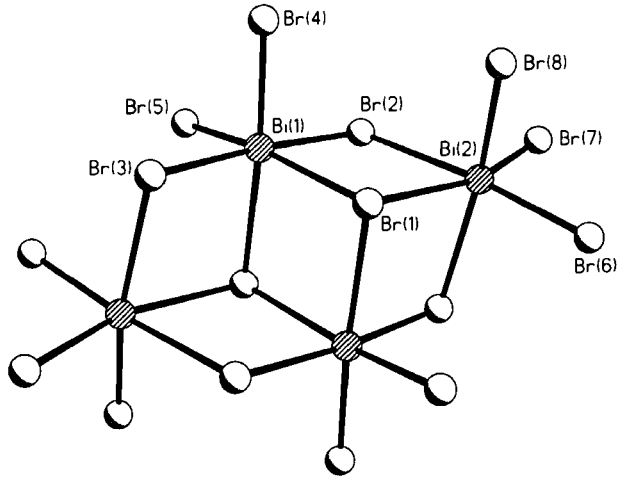


FIG. 7. The structure of $[Bi_4Br_{16}]^{4-}$ in **27**.

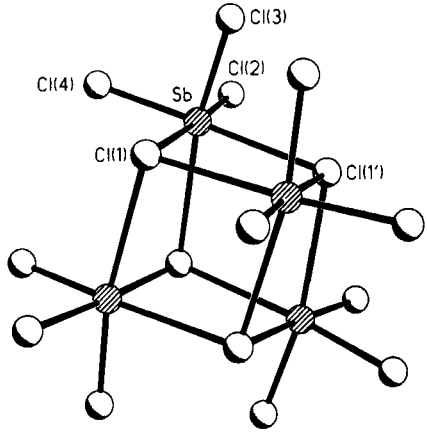


FIG. 8. The structure of $[Sb_4Cl_{16}]^{4-}$ in **28**.

perpendicular rather than parallel, as found in the previous type, shown in Fig. 7 and **G–I**. In one case there are four $\mu_3$-X groups as opposed to two $\mu_2$- and two $\mu_3$-X groups in the other. In the cubic form, the anion is isostructural with the neutral $TeCl_4$ and $TeBr_4$ structures.

The third type for which a tetramer of $[EX_4]^-$ units is an appropriate description is found in $K_4[Sb_4F_{16}]$ (**29**) (*45*), shown in Fig. 9. This is

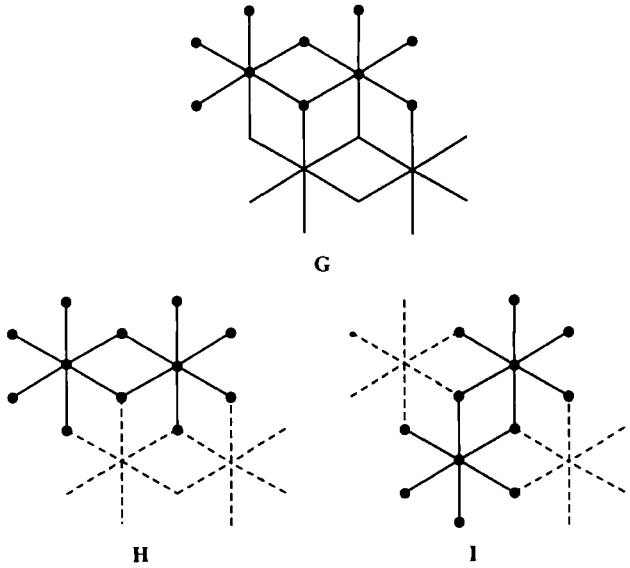

**G**

**H** **I**

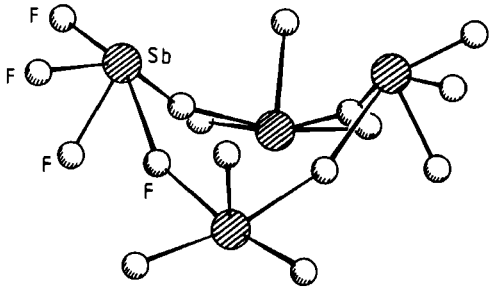


FIG. 9. The structure of $[Sb_4F_{16}]^{4-}$ in **29**.

a much more open structure in which the antimony atoms are five-coordinate with a square-based pyramidal coordination geometry.

## E. $[EX_5]^{2-}$

Turning now to a system that results from a formal addition of two halide anions to a $EX_3$ molecule, i.e., $[EX_5]^{2-}$, examples in which this unit occurs as a discrete species will be addressed first before turning to dimeric and polymeric forms. In fact, monomeric or essentially monomeric examples of $[EX_5]^{2-}$ are not particularly common, two examples being $[NH_4]_2[SbCl_5]$ (**30**) (*46*) and $K_2[SbCl_5]$ (**31**) (*47*), in which a square-based pyramidal $[EX_5]^{2-}$ unit is present, as shown in **J**. In both cases, the axial Sb–Cl distance is considerably shorter than the basal Sb–Cl lengths, although this is unsurprising because the axial bond may be viewed as a two-center, two-electron bond, whereas the basal plane is composed of two perpendicular, three-center, four-electron Cl–Sb–Cl units. These units may be symmetrical or unsymmetrical as mentioned before for primary and secondary bonds. In **30** all basal Sb–Cl lengths are about 2.62 Å, whereas in **31** one unit has nearly equal lengths of 2.622 and 2.625 Å and the other is somewhat asymmetric, with distances of 2.385 and 2.799 Å. The closest interionic Sb···Cl contacts are 3.710 and 3.881 Å.

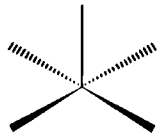

**J**

F. $[E_2X_{10}]^{4-}$

A more commonly encountered form of $[EX_5]^{2-}$ is a dimer, i.e., $[E_2X_{10}]^{4-}$, which was mentioned briefly in Section III.D. Examples include $K_4[Bi_2Br_{10}]$ (**32**) (*48*), $[NH_4]_4[Bi_2Br_{10}]$ (**33**) (*48*), $[Sr(H_2O)_8]_2[Bi_2Br_{10}]$ (**34**) (*49*), and $[HL]_4[Bi_2Br_{10}]$ (L = 2,5-diamino-1,3,4-thiadiazole) (**35**) (*50*); a view of **35** is shown in Fig. 10.

In all cases, the structure can be described as edge-shared bioctahedral and none of the interbond angles deviate from idealized values by more than a few degrees. The Bi–Br distances to the bridging bromines, in the examples given, are longer than those to the terminal bromines, as expected, but in all cases, the Bi–Br–Bi bridging units are quite symmetrical.

G. $[\{EX_5\}_n]^{2n-}$

A few examples of higher nuclearity aggregates composed of $[EX_5]^{2-}$ are known. In the structure of [2,2′-bipyridinium][$SbCl_5$] (**36**) (*51*), a tetrameric arrangement is found, as shown in **K**. Each $[SbCl_5]^{2-}$ unit is linked to two others through approximately linear chlorine bridges that are somewhat asymmetric, the relevant distances being 2.804/3.218 and 2.836/3.054 Å.

A polymeric form shown in **L** is found in [4,4′-bipyridinium][$SbCl_5$] (**37**) (*51*) and also in [piperidinium]$_2$[$BiBr_5$] (**38**) (*52*). In **37** the $[EX_5]^{2-}$ units are discernable in that the linear chlorine bridge is quite asymmetric (2.588 vs 3.182 Å), whereas in **38** the analogous Bi–Br distances

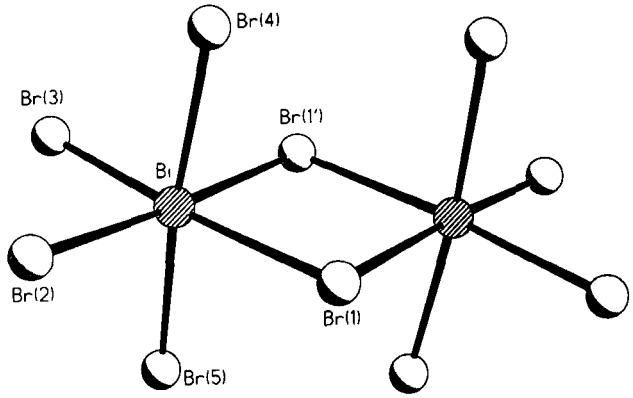


FIG. 10. The structure of $[Bi_2Br_{10}]^{4-}$ in **35**.

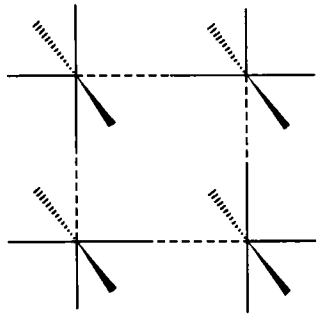

K

are more nearly symmetrical (3.02 vs 3.13 Å), such that a more regular octahedral coordination is found around the bismuth centers.

In the mixed chloride/fluoride structure $[NH_4]_2[SbCl_3F_2]$ (**39**) (*53*), a polymeric structure related to **L** is present, as shown in **M**, the main difference being that the bridging chlorides (all fluorides are terminal) are bent rather than linear, as in **L**.

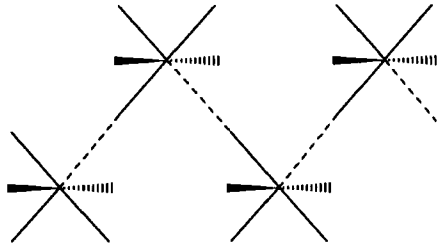

L

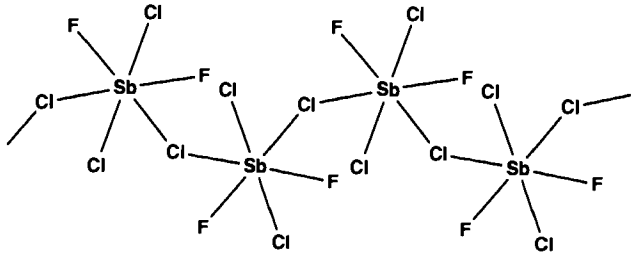


M

H. $[EX_6]^{3-}$

Formal addition of three halide ions to $EX_3$ affords the mononuclear octahedral species $[EX_6]^{3-}$. Examples include $Rb_3[BiBr_6]$ (**40**) (*54*), $[Et_2NH_2]_3[BiBr_6]$ (**41**) (*55*), $[Me_2NH_2]_3[BiBr_6]$ (**42**) (*56*), $Na_7[BiBr_6]$-

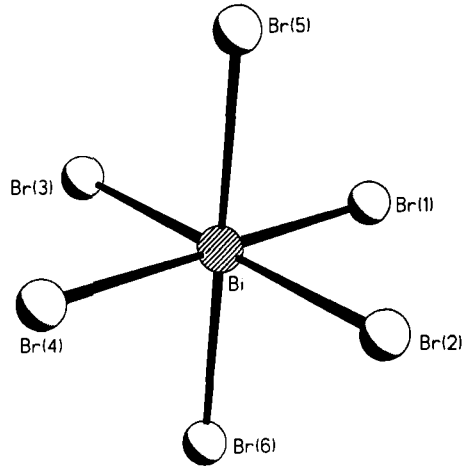


FIG. 11. The structure of $[BiBr_6]^{3-}$ in **40**.

$[Bi_2Br_{10}]\cdot 18H_2O$ (**43**) (*57*), $Cs_2Na[BiCl_6]$ (**44**) (*58*), $[Me_2NH_2]_4[BiCl_6]Cl$ (**45**) (*59*), $Rb_5[BiI_6][I_3]I\cdot 2H_2O$ (**46**) (*60*), and a range of alkali metal $[BiF_6]^{3-}$ salts (*61*); a view of **40** is shown in Fig. 11.

In general the structures of the $[EX_6]^{3-}$ ions are close to regular octahedral, with only small deviations from idealized angles and small differences in bond lengths. Such deviations as do occur tend to be of a $C_{3v}$-type distortion in which three mutually *cis* bonds are slightly longer than the bonds of their *trans* partners. The nature of these distortions will be commented upon in Section IV, when bonding is considered in a little more detail.

## I. $[E_2X_9]^{3-}$

$[E_2X_9]^{3-}$ can exist either as discrete dinuclear units, addressed here, or as polymeric forms, which are considered in the following section. The structure of the dinuclear form can be described as a confacial bioctahedron and examples include $[C_5H_5NH]_3[As_2Cl_9]$ (**47**) (*62*), $[C_5H_5NH]_3[As_2Br_9]$ (**48**) (*63*), [piperidinium]$_4[As_2Br_9]Br$ (**49**) (*64*), $[Et_2NH_2]_3[Bi_2I_9]$ (**50**) (*65*), $[Ph_4P]_3[Bi_2Br_9]$ (**51**) (*66*), $[Me_4N]_3[Sb_2Br_9]\cdot Br_2$ (**52**) (*67*), $[Me_4N]_3[Sb_2Br_9]$ (**53**) (*68*), and the mixed halide complex $[Me_4N]_3[Sb_2Cl_6(\mu\text{-}Br)_3]$ (**54**) (*68*); a view of **48** is shown in Fig. 12.

In most cases the bridging halides are quite symmetric (the exception being **49**, in which there is some degree of asymmetry) and the coordination around the group 15 element is close to that of a regular octahedron. The deviations that do occur are such that the terminal E–X bonds

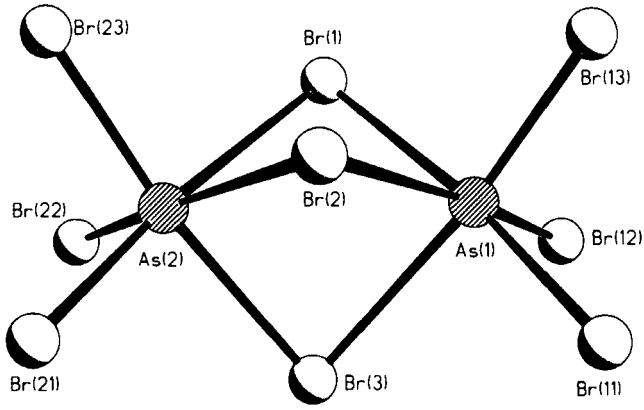


FIG. 12. The structure of $[As_2Br_9]^{3-}$ in **48**.

are shorter than the bridging E–X bonds (as expected) and also that the interbond angles at E between the terminal X groups are usually slightly greater than 90°, whereas those between the bridging X group are less than 90°. This latter distortion in angles could be interpreted as the beginnings of localization of the lone pairs *trans* to the E–E vector, but an alternative explanation is that an overall antibonding interaction between the E centers leads to a lengthening of the E–E distance with a concomitant change in the relevant bond angles. The lengths of E–E distances and the E–X–E angle for these and a series of related transition metal compounds in terms of any E–E bonding present have been addressed by Cotton and Ucko (*69*).

An alternative way of thinking about this structural type (as opposed to a confacial bioctahedron) is as an $[EX_6]^{3-}$ octahedron in which one face of the octahedron is capped by a neutral $EX_3$ unit. This is a somewhat contrived point of view but, in later sections, this capping principle will be quite useful in rationalizing a number of structural types.

One other example of a different dinuclear structure is found in $[Co(NH_3)_6][Sb_2F_9]$ (**54**) (*70*). This is a more open structure, as has been observed before for some fluoride complexes, and may be described as two square-based pyramids that share a vertex, as shown in **N**.

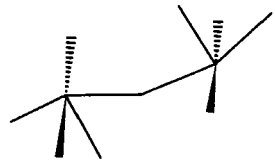

**N**

With the structure of **54** in mind, the related structure of the $[Sb_2F_7]^-$ anion should be considered, two forms of which have been observed. In $Cs[Sb_2F_7]$ (**55**) (*71*) this anion is present as a discrete dimer, with a structure as shown in **O**. A reasonable description is of two equatorially vacant, trigonal bipyramids that share an axial vertex. The terminal Sb–F bonds average about 1.95 Å, whereas the bridging Sb–F distance is 2.24 Å (a $C_2$ axis passes through the $\mu$-F atom); the Sb–F–Sb angle is 125.3°.

In the related compound $K[Sb_2F_7]$ (**56**) (*72*) discrete anions are not present and a one-dimensional polymeric structure is found, as shown in **P**. As is clear from the diagram, there are two types of antimony center, one of which is five coordinate and the other four coordinate.

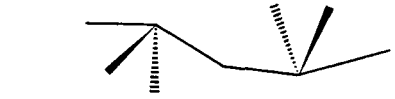

**O**

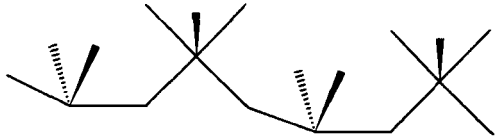

**P**

J. $[\{E_2X_9\}_n]^{3n-}$

As well as discrete dinuclear units of the form $[E_2X_9]^{3-}$, as discussed in the previous section, a number of polymeric forms are also known. The compound $[C_5H_5HN]_3[Sb_2Cl_9]$ (**57**) (*68*) has a double chain structure, as shown in Fig. 13, in which each antimony atom is octahedrally coordinated to six chlorines, three of which bridge to three different antimony centers. The structure of $[Me_3NH]_3[Sb_2Cl_9]$ (**58**) (*73*) is similar, as are the structures of $\beta$-$Cs_3[Sb_2Cl_9]$ (**59**) (*74, 75*) and $\beta$-$Cs_3[Bi_2Cl_9]$ (**60**) (*75*). In the last two, the main difference is in the packing arrangement of the double chains. Figure 13 and a discussion in Ref. *68* stress the covalent nature of the interactions between the antimony and the chlorine atoms, although the structures of **59** and **60** have been described more as an ionic type of structure involving close-packed chlorines, with the antimony atoms occupying $\frac{2}{3}$ of the octahedral holes. A comparison with the description of $BiI_3$ is interesting in this respect.

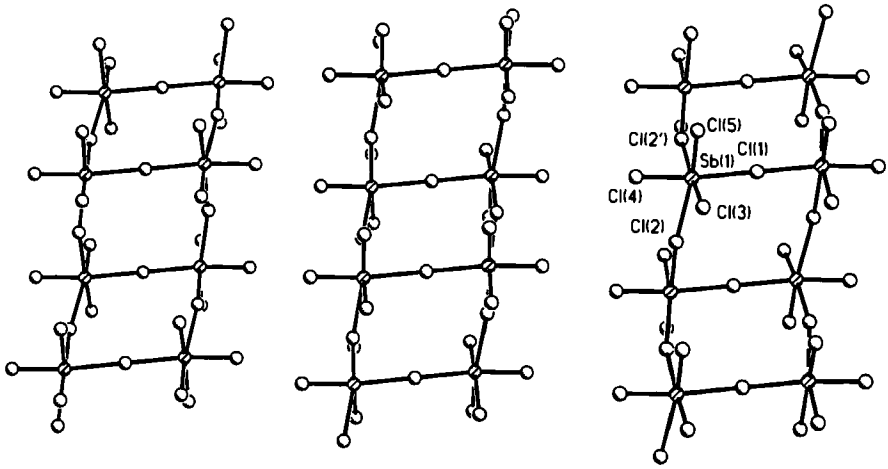


FIG. 13. Part of the polymeric structure of $[C_5H_5HN]_3[Sb_2Cl_9]$ in **57**.

Similar polymeric structures are also found in $\alpha$-$Cs_3[Sb_2Cl_9]$ (**61**) (*76*), $\alpha$-$Cs_3[Bi_2Cl_9]$ (**62**) (*75*), and $Cs_3[As_2Cl_9]$ (**63**) (*77*), which are all isomorphous, together with $Cs_3[Bi_2Br_9]$ (**64**) (*78*) and the isomorphous pair $Cs_3[Sb_2I_9]$ (**65**) (*79*) and $Cs_3[Bi_2I_9]$ (**66**) (*79*).

A different polymeric form is found in the structure of $Rb_2[SbCl_3F_2]$ (**67**) (*53*). In this case a polymeric chain of edge-shared bioctahedral units linked through linear chloride bridges, as shown in **Q**, is present, the repeat unit being $[Sb_2Cl_3F_6]^{3-}$, together with isolated $[SbCl_6]^{3-}$ octahedra and $Rb^+$ cations. A more descriptive formula is $Rb_6[Sb_2Cl_3F_6][SbCl_6]$.

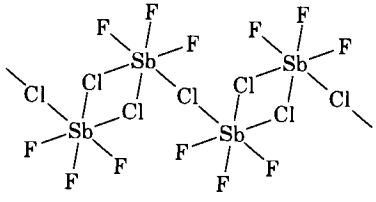


Q

## K. $[E_3X_{12}]^{3-}$

There are a number of compounds that contain discrete anions of the formula $[E_3X_{12}]^{3-}$ and these are found in two distinct forms. One

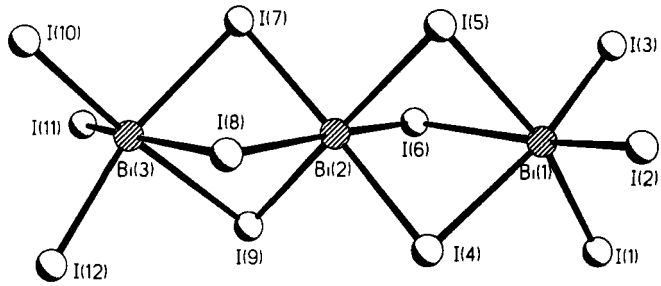


FIG. 14. The structure of $[Bi_3I_{12}]^{3-}$ in **69**.

type is what may be described as *linear* and examples include [K(15-crown-5)$_2$]$_3$[$Sb_3I_{12}$] (**68**) (*80*), [$Bu_4^nN$]$_3$[$Bi_3I_{12}$] (**69**) (*81*), and [Bi(dmpu)$_6$][$Bi_3I_{12}$] (dmpu, dimethylpropylene urea) (**70**) (*82*); a view of **69** is shown in Fig. 14. In all cases, the element E has octahedral coordination and the halides are either terminal or doubly bridging. A useful description in terms of the capping principle mentioned earlier is an $[EX_6]^{3-}$ octahedron in which two opposite faces are capped by $EX_3$ units, resulting in a threefold rotational symmetry for the anion.

A second type of $[E_3X_{12}]^{3-}$ structure is found in the complexes [$Et_3NH$]$_3$[$As_3Br_{12}$] (**71**) (*83, 84*) and [$Me_3NH$]$_3$[$As_3I_{12}$] (**72**) (*84*); a view of **72** is shown in Fig. 15. In this instance, the structure can be viewed as being derived from an $[EX_6]^{3-}$ octahedron in which two faces sharing a common vertex have been capped by $EX_3$ units. This results in termi-

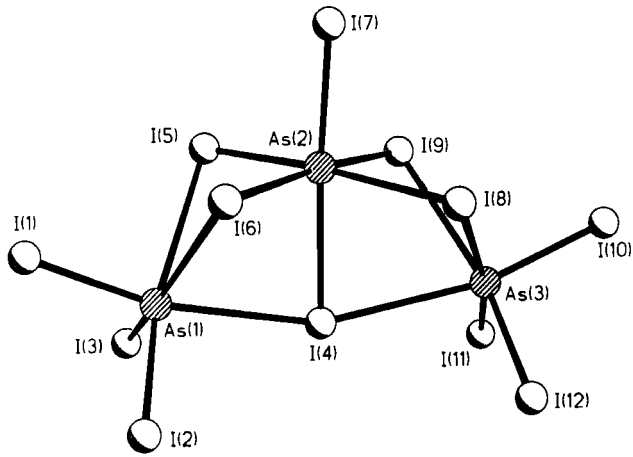


FIG. 15. The structure of $[As_3I_{12}]^{3-}$ in **72**.

nal and $\mu_2$-X groups but also in a rather unusual triply bridging halide with a T-shaped geometry.

## L. $[E_5X_{18}]^{3-}$

The capping principle can be taken a little further and used to understand a number of structures with the general formula $[E_5X_{18}]^{3-}$, three isomeric forms of which exist. The structure of $[H\{OP(NMe_2)_3\}_2]_3[Sb_5I_{18}]$ (**73**) (*85*) is shown in Fig. 16 and can be viewed as based on a central $[SbI_6]^{3-}$ octahedron in which four faces are capped by $SbI_3$ units, such that the overall structure has $D_{2h}$ symmetry. Removal of an adjacent pair of $EX_3$ units that share a common vertex (but not an edge) results in the structure type shown in Fig. 15, whereas removal of an opposite pair of $EX_3$ units results in the structure type shown in Fig. 14.

A second isomeric form is found in $[Me_4N]_3[Sb_5I_{18}]$ (**74**) (*86*), as shown in Fig. 17. This may also be viewed as an $[SbI_6]^{3-}$ octahedron associated with four $SbI_3$ units, but, in this case, it is four edges sharing a common vertex that are bridged, such that the overall structure is that of a square-based pyramid with $C_{4v}$ symmetry. Moreover, in the four $SbI_3$ units, only two of the iodines on each antimony are terminal; the others bridge to adjacent units.

A third type of structure is found in $[Ph_4P]_3[Bi_5I_{18}]$ (**75**) (*87*), in which the whole arrangement is linear with $D_{3d}$ symmetry. In this case, the structure can be built up not by capping four faces or bridging four edges of an octahedron, but by a progressive capping of the face opposite

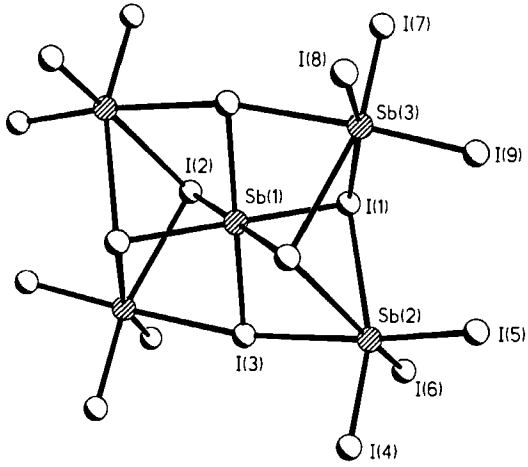


FIG. 16. The structure of $[Sb_5I_{18}]^{3-}$ in **73**.

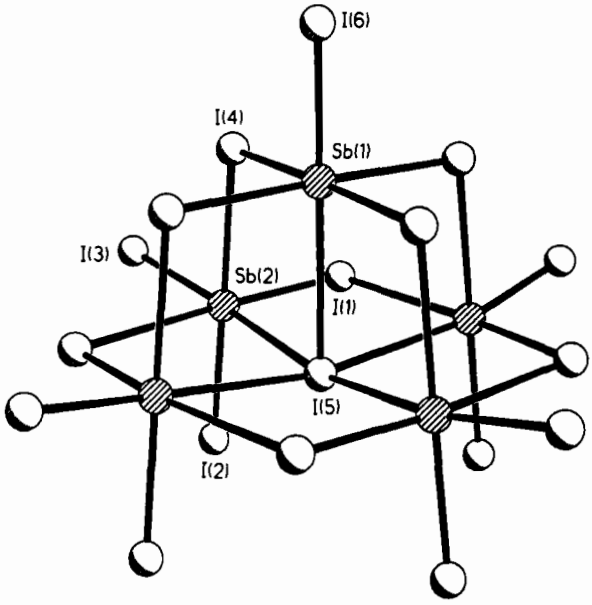


FIG. 17. The structure of $[Sb_5I_{18}]^{3-}$ in **74**.

the starting octahedron as each new $BiI_3$ unit is added. The structure is represented in **R**.

**R**

M. $[E_2X_{11}]^{5-}$

The anion $[E_2X_{11}]^{5-}$ is found in two compounds, $[MeNH_3]_5[Bi_2Br_{11}]$ (**76**) (*88*) and the isomorphous $[MeNH_3]_5[Bi_2Cl_{11}]$ (**77**) (*89*); a view of **76** is shown in Fig. 18. Both bismuth centers are octahedrally coordinated and linked by a linear halide bridge.

N. $[E_4X_{18}]^{6-}$

An anion of this formula is found in $[C_5H_5NH]_6[Bi_4Cl_{18}]$ (**78**) (*90*), the structure of which is shown in Fig. 19. Each bismuth center is

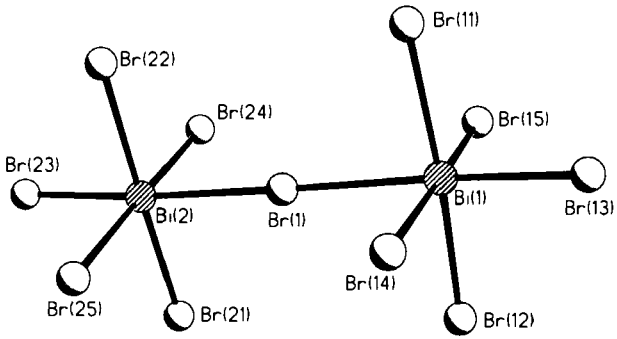


FIG. 18. The structure of $[Bi_2Br_{11}]^{5-}$ in **76**.

octahedrally coordinated and structural similarities are evident in comparison with the $[E_2X_{10}]^{4-}$ and $[E_2X_{11}]^{5-}$ structures, the latter in terms of the linear halide bridges that are present. A relationship between this unit and the polymeric structure found in **67** is also apparent.

O. $[E_3X_{11}]^{2-}$

An anion with this formula is found in $[Cu(MeCN)_4]_2[Sb_3I_{11}]$ (**79**) (*86*) and is shown in Fig. 20. Each antimony center is octahedrally coordinated, although this is somewhat distorted as a result of the four- and six-membered rings within the structure.

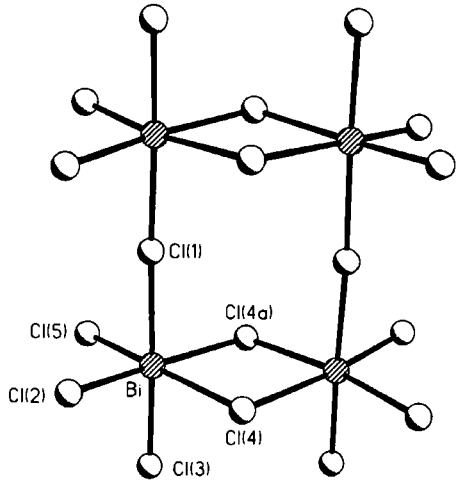


FIG. 19. The structure of $[Bi_4Cl_{18}]^{6-}$ in **78**.

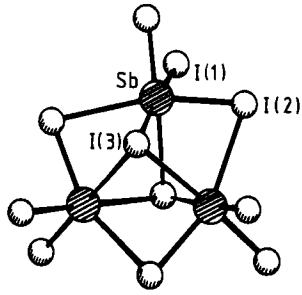


FIG. 20. The structure of $[Sb_3I_{11}]^{2-}$ in **79**.

## P. $[E_6X_{22}]^{4-}$

Hexanuclear anions of the formula $[E_6X_{22}]^{4-}$ are formally dimers of the unit encountered in **79**, although the structural similarities are not great. Three examples, which comprise two distinct but related structural forms, are known. One of these forms is found in the compounds $[Fe(\eta\text{-}C_5H_5)_2]_4[Sb_6I_{22}]$ (**80**) (*86*) and $[Et_4P]_4[Bi_6I_{22}]$ (**81**) (*91*), and a view of **80** is shown in Fig. 21. This structure can be viewed as based on the tetranuclear species $[E_4X_{16}]^{4-}$, as described in Section III.D, in which two opposite $X_3$ faces have been capped by $EX_3$ units (analogous to **I**) or, alternatively, in which the structure has been extended by addition of a further $E_2X_6$ unit (analogous to **H**). Because the $[E_4X_{16}]^{4-}$ structure can itself be viewed as being derived from the $[E_2X_{10}]^{4-}$ type, described in Section III.F, also by the addition of two $EX_3$ units (or an

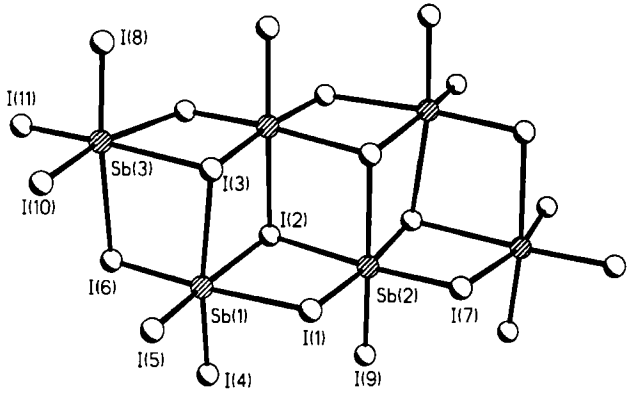


FIG. 21. The structure of $[Sb_6I_{22}]^{4-}$ in **80**.

$E_2X_6$ unit), a class of tetraanion may therefore be defined with the general formula $[E_{2n}X_{6n+4}]^{4-}$, the structures $[E_2X_{10}]^{4-}$, $[E_4X_{16}]^{4-}$, and $[E_6X_{22}]^{4-}$ forming the first three members of the series, for which $n$ = 1, 2, and 3, respectively.

The other structural form is found in the compound $[Fe(1,10\text{-phen})_3]_2$-$[Sb_6I_{22}]\cdot 2MeCN$ (**82**) (*92*), which is shown in Fig. 22. This can also be derived from the basic structure of the tetranuclear $[E_4X_{16}]^{4-}$ cluster but, whereas in **80** and **81** it is faces in the plane of the $E_4$ unit that are capped, in **82**, it is faces above and below, such that the $E_6$ core is no longer planar; Sb(3) and its symmetry related partner in Figs. 21 and 22 are the capping groups. An alternative description is a double cube that highlights a relationship between this cluster and the cubic structure of **28** in which two adjacent $EX_3$ units have been added to one face of the cube.

## Q. $[E_8X_{28}]^{4-}$

Considering the general formula $[E_{2n}X_{6n+4}]^{4-}$, described in the previous section, there are five structures known with the formula $[E_8X_{28}]^{4-}$, which extend the series to $n$ = 4. Three structural forms are known. In $[Ph_4P]_4[Sb_8I_{28}]$ (**83**) (*93*) and $[H(dmpu)_2]_4[Sb_8I_{28}]\cdot x\,C_6H_5Cl$ (**84**) (*85*), the eight antimony atoms are essentially coplanar and the structure can clearly be thought of as based on the $[E_6X_{22}]^{4-}$ cluster shown in Fig. 21, to which another two $EX_3$ units (or an $E_2X_6$ unit) have been

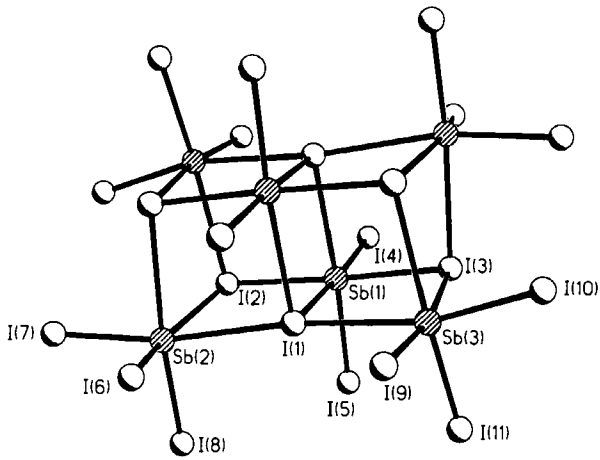


FIG. 22. The structure of $[Sb_6I_{22}]^{4-}$ in **82**.

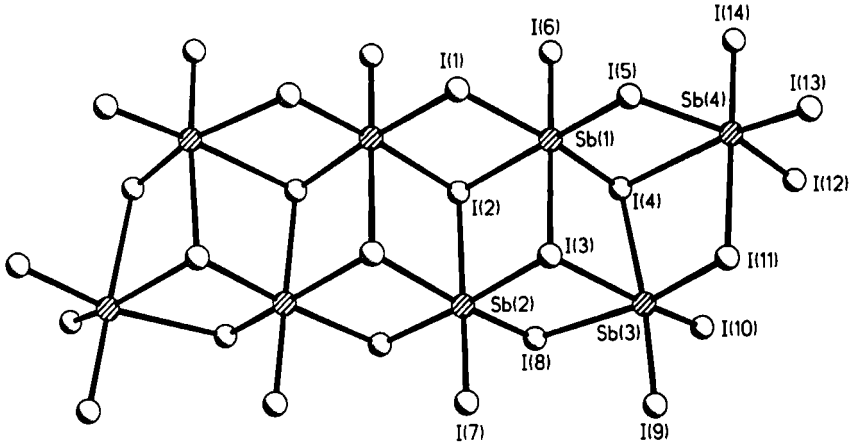


FIG. 23. The structure of $[Sb_8I_{28}]^{4-}$ in **83**.

added in much the same way as $[E_6X_{22}]^{4-}$ can be built up from $[E_4X_{16}]^{4-}$ and two $EX_3$; a view of **83** is shown in Fig. 23.

A second structural form is found in $[Me_4N]_4[Sb_8I_{28}]$ (**85**) (*94*) and $[Me_3S]_4[Sb_8I_{28}]$ (**86**) (*94*). In these cases, the structure is more three dimensional and can be thought of as built up from a $[E_4X_{16}]^{4-}$ cluster, as described in Section III.D, in which two faces are capped by $EX_3$ units, Sb(4), and two edges are bridged by $EX_3$ units, Sb(3), none of which are adjacent to each other. A view of **85** is shown in Fig. 24.

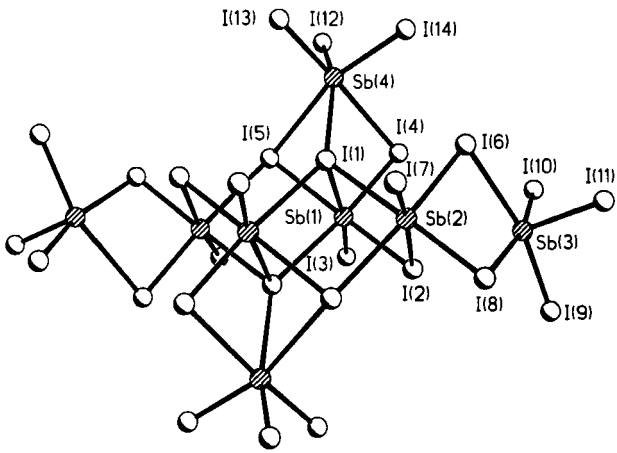


FIG. 24. The structure of $[Sb_8I_{28}]^{4-}$ in **85**.

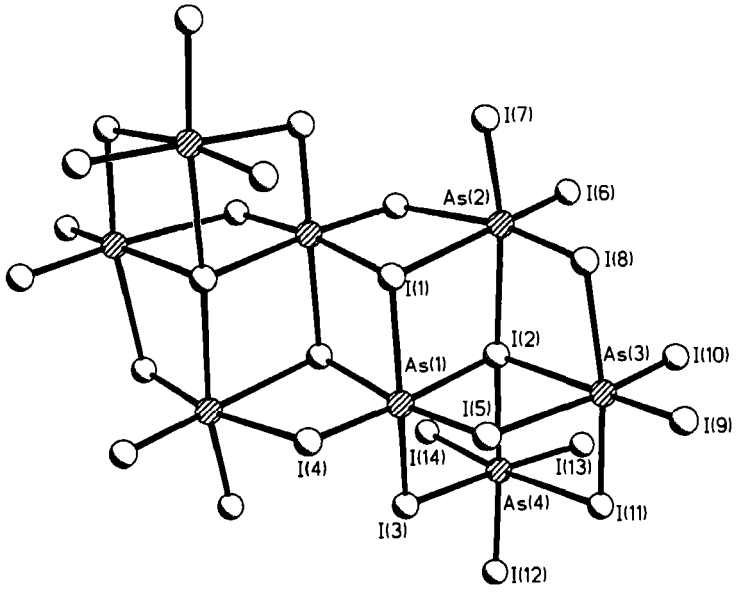


FIG. 25. The structure of $[As_8I_{28}]^{4-}$ in **87**.

A third type of structure is found in $[Et_3NH]_4[As_8I_{28}]$ (**87**) (*31*), which is shown in Fig. 25. This may also be viewed as based on an $[E_4X_{16}]^{4-}$ core in which opposite sides are bonded to $E_2X_6$ units in a way slightly different from that found in the first type of structure mentioned in this section, i.e., **83** as shown in Fig. 23. As(3) and As(4) are the atoms of the $E_2X_6$ units.

R. $[E_8X_{30}]^{6-}$

The largest discrete anion is the $[Bi_8Cl_{30}]^{6-}$ anion, found in the structure of $[Et_4N]_6[Bi_8Cl_{30}]$ (**88**) (*95*), which is shown in Fig. 26 and which has similarities to a polymeric structure described in the next section. The central unit is clearly structurally similar to the $[E_4X_{16}]^{4-}$ unit, described in Section III.D (Fig. 7), and the structure of **88** can be envisaged as built up from this core by the addition of two $[E_2X_7]^-$ anions to opposite ends.

S. $[\{E_2X_7\}_n]^{n-}$

Two structures of antimony fluorides with this empirical formula were mentioned in Section III.I because they were related to structures

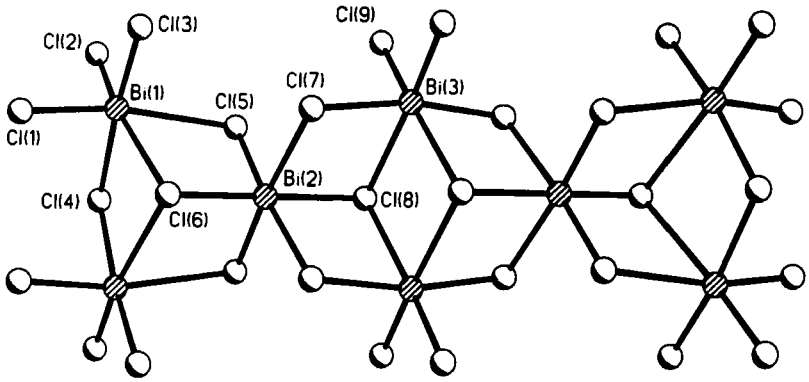


FIG. 26. The structure of $[Bi_8Cl_{30}]^{6-}$ in **88**.

discussed at that point. In this section, another example, which is found in the compound $[Me_3N(CH_2Ph)][Sb_2I_7]$ (**89**) (*94*), is considered. The anion is polymeric, is shown in Fig. 27, and is based on the $[E_4X_{16}]^{4-}$ structure (Section III.D) in such a way that the polymer can be constructed from these units by the sharing of opposite edges.

T. $[\{E_3X_{10}\}_n]^{n-}$

Three types of polymeric structure with this formula are known. A view of the anion in $[Ph_4P][Sb_3I_{10}]$ (**90**) (*93*) is shown in Fig. 28 and may be thought of as a polymer of $[E_4X_{16}]^{4-}$ units in which opposite E atoms are shared. The structural similarities to the $[Bi_8Cl_{30}]^{6-}$ anion shown in Fig. 26 are also obvious.

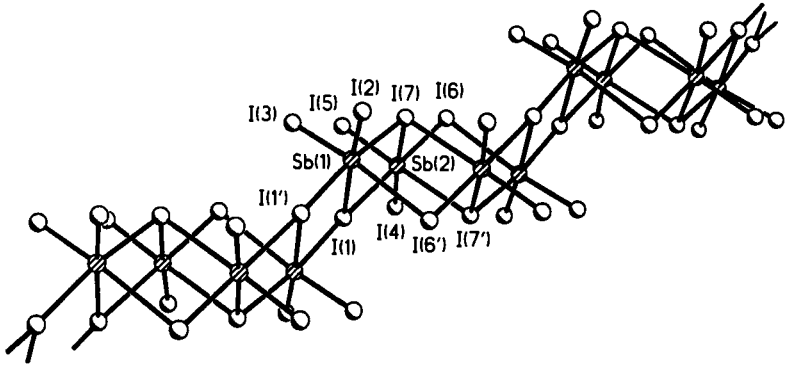


FIG. 27. Part of the polymeric structure of the $[\{Sb_2I_7\}_n]^{n-}$ anion in **89**.

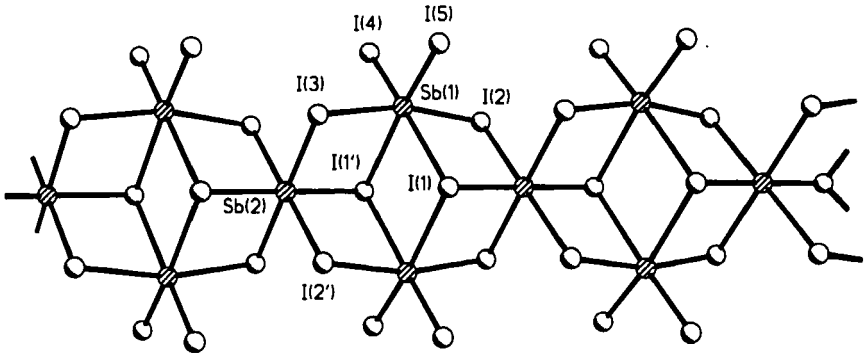


FIG. 28. Part of the polymeric structure of the $[\{Sb_3I_{10}\}_n]^{n-}$ anion in **90**.

In $[C(NMe_2)_3][Sb_3I_{10}]$ (**91**) (*96*) a different structure is found (Fig. 29). The repeat unit in this structure is derived from the $[E_6X_{22}]^{4-}$ anion shown in Fig. 21, in which opposite edges are shared in a way similar though not identical to that in which the structure of **89**, shown in Fig. 27, was derived from the $[E_4X_{16}]^{4-}$ unit.

A third structural type is observed in the structure of the fluoroantimonate complex $Na[Sb_3F_{10}]$ (**92**) (*97*), which is shown in Fig. 30. As is often found for the fluoride complexes, the structure is more open and the antimony atoms are five coordinate with a square-based pyramidal geometry. The essential unit is a triangular $[Sb_3F_9]$ fragment, with three additional fluorines, one per antimony, forming bridges to adja-

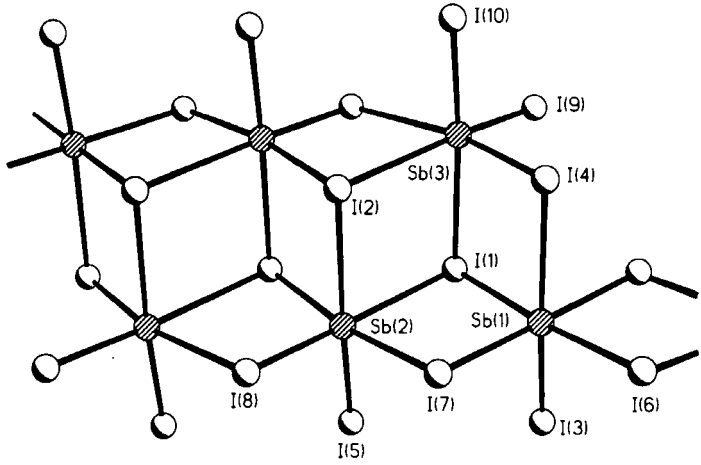


FIG. 29. Part of the polymeric structure of the $[\{Sb_3I_{10}\}_n]^{n-}$ anion in **91**.

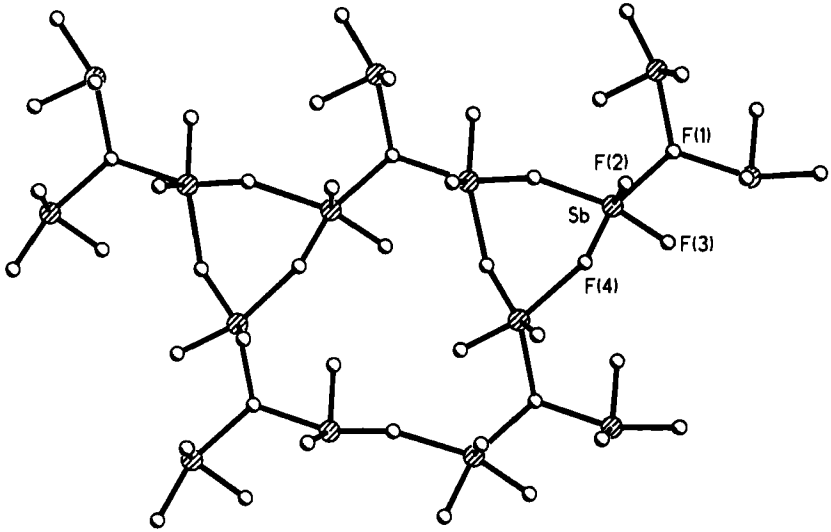


FIG. 30. Part of the polymeric structure of the $[\{Sb_3F_{10}\}_n]^{n-}$ anion in **92**.

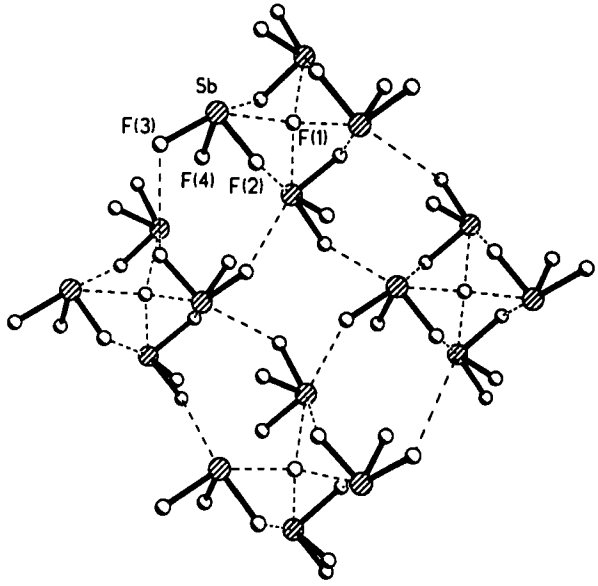


FIG. 31. Part of the polymeric structure of the $[\{Sb_4F_{13}\}_n]^{n-}$ anion in **93**.

cent triangles, such that the resulting polymeric structure is a two-dimensional infinite sheet.

### U. $[\{E_4X_{13}\}_n]^{n-}$

The complexes $Q[Sb_4F_{13}]$ (Q = K, Rb, Cs, Tl, $NH_4$) form an isomorphous series (*98*, *99*) in which the $[E_4F_{13}]^-$ unit is present as a tetramer of $SbF_3$ units, with a central fluoride anion in the center of the $Sb_4$ square and weaker Sb–F–Sb bridging interactions between the tetramers, giving rise to an infinite two-dimensional polymeric sheet. The structure of the potassium salt (**93**) is shown in Fig. 31.

## IV. General Comments

One feature that is clearly apparent from Section III is the great variety of halogenoanion structures that are known. In this regard it is interesting to note a parallel to the structural chemistry of the copper(I) halogenoanions reviewed recently by Jagner and Helgesson (*100*). These authors comment on the wide range of structures and the possible factors that affect the particular type that is formed. Of the many possible factors that might influence the solid-state structure of a given anion, undoubtedly the most important is the nature of the cation, such as the size, shape, and localization of charge. These features are not easy to quantify and it is therefore difficult if not impossible to predict or rationalize many of the observed structures, but a number of general points do emerge. For example, Jagner and Helgesson comment on the fact that the smaller copper(I) halogenoanions are generally associated with smaller cations, i.e., that the anion size and the cation size (or collective size of the cations if more than one is needed to balance the charge of the anion) tend to be similar. The importance of ion size and shape has been addressed in general terms by Mingos and Rohl (*101*), and a useful discussion of the importance of relative ion sizes with respect to lattice energies has been given by Alcock (*18*). Nevertheless, the difficulties associated with any rationalizations are clear if a number of structures mentioned in Section III are compared. For example, compounds **15** and **26** have the same $[Mg(MeCN)_6]^{2+}$ cation but, in the former case, the $[SbCl_4]^-$ anion is polymeric, whereas, in the latter case, the $[BiCl_4]^-$ anion is a tetramer. A similar situation is observed for **17**, with a polymeric $[BiCl_4]^-$ anion, and **27**, with a tetrameric $[BiBr_4]^-$ anion, the cation in both these cases being $[Fe(\eta$-

$C_5H_5)_2]^+$. Moreover, in **80**, four $[Fe(\eta\text{-}C_5H_5)_2]^+$ cations are associated with the $[Sb_6I_{22}]^{4-}$ anion rather than a tetrameric $[Bi_4Br_{16}]^{4-}$ anion, as found in **27**. There are many other pairs of structures that differ in having the same number and type of cation but different anion structures, e.g., **47/57** and **41/50**, which further illustrate this point. Factors such as the solvent and concentration of the reactants are also probably important in determining the type of structure that crystallizes; as is found in the copper(I) chemistry, the species present in solution are probably simple mononuclear or dinuclear units. It should be borne in mind that many of the structures formed may be determined as much by the kinetics of crystallization as by thermodynamic factors.

Turning now to the structures themselves, it is worth reiterating the point, made in Section II, that, as with the halides themselves, the structures of the anions reveal strongly correlated *trans* bond lengths and that the primary and secondary bond lengths are generally more nearly equal the heavier the elements involved. This feature is also related to the degree of bridge asymmetry in $E_2(\mu\text{-}X)_2$ units, which tends to be greatest for chlorides and least for iodides, although in polymeric structures there may be considerable variation in the asymmetry of adjacent bridging units.

With regard to coordination geometries, it is clear that, despite the wide variety of structural types, in the vast majority of cases the group 15 element is six coordinate and that the coordination geometry is close to octahedral. This raises the problem, alluded to earlier, of the stereochemical activity or significance of the lone pair of electrons that is present in all element(III) complexes.

In the four- and five-coordinate structures, there is little problem in understanding the coordination geometry; the structures are as predicted by VSEPR theory and are also consistent with the $\sigma^*$-orbital model for Lewis acidity outlined in Section II. Thus in **1**, for example, the equatorially vacant trigonal bipyramidal structure is anticipated from VSEPR but the anion can also be understood as a complex of $PCl_3$ and $Cl^-$ in which the $Cl^-$ interacts with one P–Cl $\sigma^*$-orbital, which leads to a lengthening of the P–Cl bond *trans* to the coordinated chloride. In **2** the axial P–Br bonds are more nearly the same length as the distinction between primary and secondary becomes less distinct, but both are longer than the bonds to the terminal bromines. Also, the beginnings of five coordination, which leads to a square-based pyramidal geometry as a second $\sigma^*$-orbital is employed, are apparent. The way in which four- and five-coordinate structures can be built up from a trigonal pyramid is illustrated by considering one and two $X^-$ groups, respectively, in **S**, where the lobes represent the E–X $\sigma^*$-orbitals.

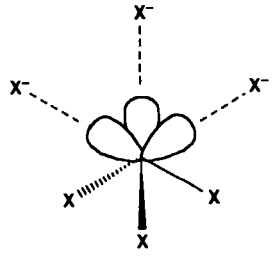


S

In the vast majority of cases in which six coordination is observed, the bonding can be viewed as arising from the interaction of all three $\sigma^*$-orbitals with a halide anion, i.e., all three $X^-$ in **S**. Because the three orbitals are all *trans* to the primary E–X bonds, such a situation leads naturally to octahedral coordination. Moreover, in cases in which the primary and secondary bonds are the same length, i.e., where $\Delta = 0$ and a three-center, four-electron bonding model is appropriate, a regular octahedron is the result. Such a structure is clearly at odds with simple VSEPR theory, which is predicated on the lone pair(s) occupying specific stereochemical sites, but stereochemical inactivity of the lone pair tends to be the rule rather than the exception in six-coordinate, seven-electron pair systems; Ng and Zuckerman (*102*) have reviewed this topic for *p*-block compounds in general.

The problem of stereochemical activity of lone pairs is, in fact, more subtle than either of the simplified models outlined above, and this point can be illustrated with reference to some specific examples. Thus, in an illuminating paper, Wheeler and Kumar (*103*) comment on the fact that in compound **46**, the $[BiI_6]^{3-}$ octahedron is regular (undistorted), whereas, in $[H_3N(CH_2)_3NH_3]_3[BiCl_6]_2{\cdot}2H_2O$ (**94**) (*104*), the $[BiCl_6]^{3-}$ octahedron shows a marked trigonal $C_{3v}$ distortion in which three angles are slightly less than 90° and three are slightly greater. Furthermore, the three mutually *cis* Bi–Cl bonds in **94** that have interbond angles greater than 90° are significantly longer than the other three (2.644 vs 2.792 Å), both of these factors being consistent with the beginnings of lone pair localization in this face of the octahedron. In **94** and in the isomorphous bromide complex, the beginnings of stereochemical activity of the lone pair, which is clearly inactive in **46**, is evident.

An extended Hückel molecular orbital analysis on both of these complexes revealed that this structural difference between the chloride and the iodide can be traced to a second-order Jahn–Teller distortion, which is predicted to occur more readily for the chloride. Specifically,

the calculations indicate that the relevant orbital mixing (which will not be discussed in detail here) is expected to be greater in an octahedral chloride, as opposed to an iodide, because the relevant orbitals are closer in energy, with the result that the chlorides should show a greater tendency to be distorted, as is indeed observed. Furthermore, this distortion is expected to take place along a $C_{3v}$ coordinate, through changes either in bond angles or in bond lengths, precisely as seen in **94**.[1] This distortion is associated with the onset of the stereochemical activity of the lone pair, which becomes localized on one face of the octahedron. Moreover, a $C_{3v}$ distortion is predicted to be of lower energy than any alternative modes, such as localization of the lone pair along one edge of the octahedron with a concomitant enlargement of one angle: a $C_{2v}$ distortion.

It should be borne in mind that the difference in energy between distorted and undistorted structures is likely to be small and of the same order as crystal packing forces; for example, the $[BiCl_6]^{3-}$ anion in **44** is a regular octahedron and it should be anticipated that changes in the cation will have significant effects. Nevertheless, the trend is clear in that more regular coordination geometries should be expected for the iodides, in terms of both bond lengths and bond angles, which is broadly in line with what is observed.

Similar arguments can be advanced to account for why bismuth halides and halogenoanions have more regular geometries than arsenic or antimony systems. In this regard, Wheeler and Kumar carried out calculations on the solid-state structures of $BiI_3$ and $SbI_3$. As will be recalled from Section II, these two solids (and $AsI_3$) are isomorphous and differ only in the degree to which the group 15 element center is displaced toward three mutually *cis* iodides. The degree of distortion increases from Bi to As and this is also traced to a second-order Jahn–Teller distortion, which becomes more pronounced for the lighter element. In this case, the distortion is manifest not only as an asymmetry in the E–I distances but also as a *decrease* in the interbond angles between the longer E–I bonds (and a corresponding increase in the angles between the shorter bonds), the opposite of what is observed in molecular species. This results from the constraints imposed on the

[1] A distinction should be made between two variations of this $C_{3v}$ distortion. In one case, an increase in the angles of three mutually *cis* E–X bonds may occur without any significant changes in bond lengths. Alternatively, three mutually *cis* E–X bonds may lengthen without a significant change in any bond angles. Combinations of both are, of course, possible and these types of change account for most of the observed distortions from regular octahedral geometry.

iodide positons by the solid lattice and is an unusual example of a lone pair becoming localized in a region of decreasing bond angles.

In conclusion, these studies provide a theoretical foundation for rationalizing many of the trends in coordination geometry regularity (bond lengths and angles), which have been commented upon throughout this chapter. More simplified descriptions of second-order Jahn–Teller distortions in some of these systems can be found in Refs. *105* and *106*.

ACKNOWLEDGMENTS

We thank A. G. Orpen, S. Pohl, and W. S. Sheldrick for their comments and for sharing results prior to publication.

REFERENCES

1. Gillespie, R. J., Slim, D. R., and Vekris, J, E., *J. Chem. Soc., Dalton Trans.*, 971 (1977); Edwards, A. J., and Slim, D. R., *J. Chem. Soc., Chem. Commun.*, 178 (1974).
2. Davidovich, R. L., and Buslaev, Y., *Koord. Chem.* **14,** 1011 (1988).
3. Sawyer, J. F., and Gillespie, R. J., *Prog. Inorg. Chem.* **34,** 65 (1986).
4. Wells, A. F., "Structural Inorganic Chemistry," 5th ed. Oxford Univ. Press, Oxford, 1984.
5. Müller, U., "Inorganic Structural Chemistry," Wiley, Chichester, 1992.
6. Edwards, A. J., *J. Chem. Soc. A,* 2751 (1971).
7. Gries, O., and Martinez-Ripoll, M., *Z. Anorg. Allg. Chem.* **436,** 105 (1977); Cheetham, A. K., and Norman, N., *Acta. Chem. Scand. A* **28,** 55 (1974).
8. Lipka, A., *Acta Crystallogr. B* **35,** 3020 (1979).
9. Cushen, D. W., and Hulme, R., *J. Chem. Soc.*, 2218 (1962).
10. Nyburg, S. C., Ozin, G. A., and Szymanski, J. T., *Acta Crystallogr. B* **27,** 2298 (1971).
11. Cushen, D. W., and Hulme, R., *J. Chem. Soc.*, 4162 (1964).
12. Trotter, J., *Z. Kristallogr.* **122,** 230 (1965).
13. von Benda, H., *Z. Kristallogr.* **151,** 271 (1980).
14. Pohl, S., and Saak, W., *Z. Kristallogr.* **169,** 177 (1984).
15. Trotter, J., and Zobel, T., *Z. Kristallogr.* **123,** 67 (1966).
16. Enjalbert, R., and Galy, J., *Acta Crystallogr. B.* **36,** 914 (1980).
17. Alcock, N. W., *Adv. Inorg. Chem. Radiochem.* **15,** 1 (1972).
18. Alcock, N. W., "Bonding and Structure: Structural Principles in Inorganic and Organic Chemistry." Ellis Horwood, Chichester, 1990.
19. Sheldrick, W. S., and Martin, C., *Z. Naturforsch. B* **46,** 639 (1991); James, M. A., Knop, O., and Cameron, T. S., *Can. J. Chem.* **70,** 1795 (1992); Krebs, B., and Ahlers, F.-P., *Adv. Inorg. Chem.* **35,** 235 (1990).
20. Clegg, W., Compton, N. A., Errington, R. J., Fisher, G. A., Hockless, D. C. R., Norman, N. C., Williams, N. A. L., Stratford, S. E., Nichols, S. J., Jarrett, P. S., and Orpen, A. G., *J. Chem. Soc., Dalton Trans.*, 193 (1992); Clegg, W., Errington,

R. J., Fisher, G. A., Hockless, D. C. R., Norman, N. C., Orpen, A. G., and Stratford, S. E., *J. Chem. Soc., Dalton Trans.*, 1967 (1992); Clegg, W., Errington, R. J., Fisher, G. A., Flynn, R. J., and Norman, N. C., *J. Chem. Soc., Dalton Trans.*, 637 (1993), and references therein.

21. Dillon, K. B., Platt, A. W. G., Scmidpeter, A., Zwaschka, F., and Sheldrick, W. S., *Z. Anorg. Allg. Chem.* **488,** 7 (1982).
22. Sheldrick, W. S., Scmidpeter, A., Zwaschka, F., Dillon, K. B., Platt, W. G., and Waddington, T. C., *J. Chem. Soc., Dalton Trans.*, 413 (1981).
23. Kaub, J., and Sheldrick, W. S., *Z. Naturforsch. B* **39,** 1252 (1984).
24. Sheldrick, W. S., and Horn, C., *Z. Naturforsch. B* **44,** 405 (1989).
25. Sheldrick, W. S., and Kiefer, J., *Z. Naturforsch. B* **47,** 1079 (1992).
26. Pohl, S., Saak, W., and Haase, D., *Angew. Chem., Int. Ed. Engl.* **26,** 467 (1987).
27. Belz, J., Weber, R., Roloff, A., and Ross, B., *Z. Kristallogr.* **202,** 281 (1992).
28. Alcock, N. W., Ravindran, M., and Willey, G. R., *J. Chem. Soc., Chem. Commun.*, 1063 (1989).
29. Ensinger, U., Schwarz, W., and Schmidt, A., *Z. Naturforsch. B* **37,** 1584 (1982).
30. Kaub, J., and Sheldrick, W. S., *Z. Naturforsch. B* **39,** 1257 (1984).
31. Sheldrick, W. S., Häusler, H.-J., and Kaub, J., *Z. Naturforsch. B* **43,** 789 (1988).
32. Porter, S. K., and Jacobson, R. A., *J. Chem. Soc. A*, 1356 (1970).
33. Drew, M. G. B., Claire, P. P. K., and Willey, G. R., *J. Chem. Soc., Dalton Trans.*, 215 (1988).
34. Blazic, B., and Lazarini, F., *Acta Crystallogr. C* **41,** 1619 (1985).
35. Mammano, N. J., Zalkin, A., Landers, A., and Rheingold, A. L., *Inorg. Chem.* **16,** 297 (1977).
36. Robertson, B. K., McPherson, W. G., and Meyers, E. A., *J. Phys. Chem.* **71,** 3531 (1967).
37. Habibi, N., Bonnet, B., and Ducourant, B., *J. Fluorine Chem.* **12,** 237 (1978).
38. Habibi, N., Ducourant, B., Bonnet, B., and Fourcade, R., *J. Fluorine Chem.* **12,** 63 (1978).
39. Ducourant, B., Fourcade, R., Philippot, E., and Mascherpa, G., *Rev. Chim. Miner.* **12,** 485 (1975).
40. Ducourant, B., Fourcade, R., and Mascherpa, G., *J. Fluorine Chem.* **11,** 149 (1978); *Rev. Chim. Miner.* **20,** 314 (1983).
41. Aurivillus, B., and Lindblom, C.-I., *Acta Chem. Scand.* **18,** 1554 (1964).
42. Antolini, L., Benedetti, A., Fabretti, A. C., and Giusti, A., *J. Chem. Soc., Dalton Trans.*, 2501 (1988).
43. Willey, G. R., Collins, H., and Drew, M. G. B., *J. Chem. Soc., Dalton Trans.*, 961 (1991).
44. Rheingold, A. L., Uhler, A. D., and Landers, A. G., *Inorg. Chem.* **22,** 3255 (1983).
45. Byström, A., Bäcklund, S., and Wilhelmi, K.-A., *Ark. Kemi.* **4,** 175 (1952).
46. Edstrand, M., Inge, M., and Ingri, N., *Acta Chem. Scand.* **9,** 122 (1955).
47. Wismer, R. K., and Jacobson, R. A., *Inorg. Chem.* **13,** 1678 (1974).
48. Lazarini, F., *Acta Crystallogr. B* **33,** 1954 (1977).
49. Lazarini, F., and Leban, I., *Acta Crystallogr. B* **36,** 2745 (1980).
50. Benedetti, A., Fabretti, A. C., and Malavasi, W., *J. Crystallogr. Spectrosc. Res.* **22,** 145 (1992).
51. Lipka, A., *Z. Naturforsch. B* **38,** 1615 (1983).
52. McPherson, W. G., and Meyers, E. A., *J. Phys. Chem.* **72,** 532 (1968).
53. Udovenko, A. A., Volkova, L. M., and Davidovich, R. L., *Sov. J. Coord. Chem.* (*Engl. Transl.*) **4,** 234 (1978).

54. Lazarini, F., *Acta Crystallogr. B* **34,** 2288 (1978).
55. Lazarini, F., *Acta Crystallogr. C* **41,** 1617 (1985).
56. McPherson, W. G., and Meyers, E. A., *J. Phys. Chem.* **72,** 3117 (1968).
57. Lazarini, F., *Acta Crystallogr. B* **36,** 2748 (1980).
58. Morss, L. R., and Robinson, W. R., *Acta Crystallogr. B* **28,** 653 (1972).
59. Herdtweck E., and Kreusel, U., *Acta Crystallogr. C* **49,** 318 (1993).
60. Lazarini, F., *Acta Crystallogr. B* **33,** 1957 (1977).
61. Coussin, A., Vedrine, A., and Cousseins, J.-C., *C.R. Acad. Sci. Paris* **274,** 864 (1972).
62. Kaub, J., and Sheldrick, W. S., *Z. Naturforsch. B* **39,** 1252 (1984).
63. Kaub, J., and Sheldrick, W. S., *Z. Naturforsch. B* **39,** 1257 (1984).
64. Sheldrick, W. S., and Horn, C., *Z. Naturforsch. B* **44,** 405 (1989).
65. Lazarini, F., *Acta Crystallogr. C* **43,** 875 (1987).
66. Lazarini, F., *Acta Crystallogr. B* **33,** 2686 (1977).
67. Hubbard, C. R., and Jacobson, R. A., *Inorg. Chem.* **11,** 2247 (1972).
68. Hall, M., Nunn, M., Begley, M. J., and Sowerby, B. D., *J. Chem. Soc., Dalton Trans.,* 1231 (1986).
69. Cotton, F. A., and Ucko, D. A., *Inorg. Chim. Acta* **6,** 161 (1972).
70. Schroeder, D. R., and Jacobson, R. A., *Inorg. Chem.* **12,** 515 (1973).
71. Ryan, R. R., Mastin, S. H., and Larson, A. C., *Inorg. Chem.* **10,** 2793 (1971).
72. Mastin, S. H., and Ryan, R. R., *Inorg. Chem.* **10,** 1757 (1971).
73. Kruger, F. J., Zettler, F., and Schmidt, A., *Z. Anorg. Allg. Chem.* **449,** 135 (1978).
74. Kihara, K., and Sudo, T., *Acta Crystallogr. B* **30,** 1088 (1974).
75. Meyer, G., and Schönemund, A., *Z. Anorg. Allg. Chem.* **468,** 185 (1980).
76. Kihara, K., and Sudo, T., *Z. Kristallogr.* **134,** 142 (1971).
77. Howard, J. L., and Goldstein, L., *J. Chem. Phys.* **3,** 117 (1935).
78. Lazarini, F., *Acta Crystallogr. B* **33,** 2961 (1977).
79. Chalbot, B., and Parthe, E., *Acta Crystallogr. B* **34,** 645 (1978).
80. Borgsen, B., Weller, F., and Dehnicke, K., *Z. Anorg. Allg. Chem.* **596,** 55 (1991).
81. Gieser, U., Wade, E., Wang, H. H., and Williams, J. M., *Acta Crystallogr. C* **46,** 1547 (1990).
82. Carmalt, C. J., Farrugia, L. J., and Norman, N. C., submitted for publication.
83. Sheldrick, W. S., and Häusler, H.-J., *Angew. Chem., Int. Ed. Engl.* **26,** 1172 (1987).
84. Sheldrick, W. S., and Kiefer, J., *Z. Naturforsch. B* **47,** 1079 (1992).
85. Carmalt, C. J., Farrugia, L. J., and Norman, N. C., *Polyhedron* **12,** 2081 (1993).
86. Pohl, S., Lotz, R., Saak, W., and Haase, D., *Angew. Chem., Int. Ed. Engl.* **28,** 344 (1989).
87. Pohl, S., personal communication.
88. Matuszewski, J., Jakubas, R., Sobczyk, L., and Glowiak, T., *Acta Crystallogr. C* **46,** 1385 (1990).
89. Lefebvre, J., Carpenter, P., and Jakubas, R., *Acta Crystallogr. B* **47,** 228 (1991).
90. Aurivillius, B., and Stalhandske, C., *Acta Chem. Scand. A* **32,** 715 (1978).
91. Clegg, W., Errington, R. J., Fisher, G. A., Green, M. E., Hockless, D. C. R., and Norman, N. C., *Chem. Ber.* **124,** 2457 (1991).
92. Pohl, S., Haase, D., Lotz, R., and Saak, W., *Z. Naturforsch. B* **43,** 1033 (1988).
93. Pohl, S., Saak, W., and Haase, D., *Z. Naturforsch. B* **42,** 1493 (1987).
94. Pohl, S., Lotz, R., Haase, D., and Saak, W., *Z. Naturforsch. B* **43,** 1144 (1988).
95. Zaleski, J., Glowiak, T., Jakubas, R., and Sobczyk, L., *J. Phys. Chem. Solids* **50,** 1265 (1989).
96. Pohl, S., Saak, W., Mayer, P., and Schmidpeter, A., *Angew. Chem., Int. Ed. Engl.* **25,** 825 (1986).

*97.* Fourcade, R., Mascherpa, G., and Philippot, E., *Acta Crystallogr. B* **31,** 2322 (1975).
*98.* Byström, A., and Wilhelmi, K.-A., *Ark. Kemi.* **3,** 17 (1951).
*99.* Ducourant, B., Fourcade, R., Philippot, E., and Mascherpa, G., *Rev. Chim. Miner.* **12,** 553 (1975).
*100.* Jagner, S., and Helgesson, G., *Adv. Inorg. Chem.* **37,** 1 (1991).
*101.* Mingos, D. M. P., and Rohl, A. L., *J. Chem. Soc., Dalton Trans.,* 3419 (1991).
*102.* Ng, S. W., and Zuckerman, J. J., *Adv. Inorg. Chem. Radiochem.* **29,** 297 (1985).
*103.* Wheeler, R. A., and Kumar, P. N. V. P., *J. Am. Chem. Soc.* **114,** 4776 (1992).
*104.* du Bois, A., and Abriel, W., *Z. Naturforsch. B* **43,** 1003 (1988); du Bois, A., and Abriel, W., *Z. Kristallogr.* **182,** 36 (1988).
*105.* Gimarc, B. M., "Molecular Structure and Bonding." Academic Press, New York, 1979.
*106.* Albright, T. A., Burdett, J. K., and Whangbo, M. H., "Orbital Interactions in Chemistry." Wiley–Interscience, New York, 1985.

## NOTE ADDED IN PROOF

Since the submission of this chapter some additional halogenoanion structural types have been characterized. A third structure type for the $[E_6X_{22}]^{4-}$ anion (Section III.P) has been found in the isomorphous pair of compounds $[Et_3N(CH_2Ph)]_4[E_6I_{22}]$ (E = Sb, Bi) (**95**) (*107*). This structure can also be derived from the $[E_4X_{16}]^{4-}$ structure (Section III.D) and two $EX_3$ units, but in which the $EX_3$ units cap $X_3$ faces in a manner different from that encountered in the structures shown in Fig. 21 (**80**) and in Fig. 22 (**82**). The relationship between all three structural types is discussed in (*107*). A fourth structural type of the $[E_8X_{28}]^{4-}$ anion is observed in the structure of $[CH_3(CH_2)_2COS(CH_2)_2NMe_3]_4[Sb_8I_{28}]$ (**96**) (*108*), which can be derived from the structure of the double cubic $[E_6X_{22}]^{4-}$ anion in **82** in which two opposite $X_2$ edges have been bridged by $SbI_3$ units. Finally, a polymeric iodoantimonate anion is found in the structure of [2-(4-nitrophenyl)allyl]trimethylammonium][$Sb_3I_{10}$] (**97**) (*109*). The empirical formula of the anion is the same as those discussed in Section III.T, although the structure is quite different, comprising a polymer in which some of the six antimony atoms in the repeat unit, $[Sb_6I_{20}]^{2-}$, are disordered between the seven available octahedral interstices of the close-packed iodine atom array.

*107.* Pohl, S., Peters, M., Haase, D., and Saak, W., *Z. Naturforsch. B,* in press.
*108.* Carmalt, C.J., Farrugia, L.J., and Norman, N. C., *Z. Anorg. Allg. Chem.,* in press.
*109.* Carmalt, C. J., Farrugia, L. J., and Norman, N. C., *Polyhedron,* in press.